Plasmonics (2013) 8:523–527
DOI 10.1007/s11468-012-9426-5

Tip-Enhanced Ultrasensitive Stokes and Anti-Stokes Raman Spectroscopy in High Vacuum

Zhenglong Zhang · Xiaorui Tian · Hairong Zheng · Hongxing Xu · Mengtao Sun

Received: 9 May 2012 / Accepted: 6 August 2012 / Published online: 14 August 2012

Abstract We report ultrasensitive Stokes and anti-Stokes Raman spectra of 1,2-benzenedithiol monolayer on Ag film with home-made high-vacuum tip-enhanced Raman spectroscopy (HV-TERS) system. Raman peaks that were orginally very weak were observed experimentally and assigned theoretically. The local temperature was obtained based on the observed Stokes and anti-Stokes HV-TERS spectra.

Keywords TERS · Plasmon resoance · Nanogap · Polarization

Introduction

Firstly demonstrated by Stöckle, Hayazawa and Anderson in 2000 [1–3], tip-enhanced Raman spectroscopy (TERS), is an essential analytical tool with extremely high optical sensitivity. The sharp metal tip as a controlled plasmon antenna excites the localized surface plasmons and consequently enhances the electromagnetic field in the vicinity of the tip apex in the TERS system [1–13]. TERS can offer a nanoscale resolution beyond the diffraction limit of light as well because the enhanced Raman signals are from the very tiny tip area with the size of tens nanometers. In general, the tiny tip simultaneously acts as a tip of a scanning tunneling microscope (STM), atomic force microscope, or scanning near-field optical microscope device [1]. In order to extend the TERS applicability, it is best that the STM unit and the optical system are mounted on the same vibration isolated platform that is located in a vacuum chamber. Moreover, since high vacuum can give clean chemical environments that favors to vibrational analysis, it is mandatory to build up TERS in high-vacuum system to achieve a novel resolution for finger print vibrational analysis. However, it is a great challenge to cooperate an optical system with a high-vacuum system to achieve highly efficient illumination and collection of extremely weak Raman signals. The most severe restriction in the application of surface-enhanced Raman scattering (SERS) is that it requires roughness or aggregated metal nanostructures to create "hot sites", which is hardly controlled in practice. While a high-vacuum TERS (HV-TERS) can avoid this restriction, it has advantages to a wide variety of problems in single crystal surface science, electrochemistry, heterogeneous catalysis, and microelectronics [6, 9, 10].

It is expected that Raman spectra would gain more convincing spectroscopic finger print evidence if more weak vibrational modes as well as strong vibrational modes were simultaneously observed. Moreover, experimentally measuring and monitoring the in situ temperature has great significance for temperature-dependent spectrum analysis, molecular catalytic reaction, high Tc superconductor, and molecular biology [14–16]. By using Boltzmann distribution theory, Stokes and anti-Stokes Raman spectra could let us estimate the in situ local temperature [17] and study the molecular vibrational redistribution by ultrafast Raman [18]. However, it is hard to

Z. Zhang · X. Tian · H. Xu · M. Sun (✉)
Beijing National Laboratory for Condensed Matter Physics,
Institute of Physics, Chinese Academy of Sciences,
Beijing 100190, People's Republic of China
e-mail: mtsun@aphy.iphy.ac.cn

Z. Zhang · H. Zheng
College of Physics and Information Technology,
Shaanxi Normal University,
Xi'an 710062, People's Republic of China

H. Xu
Division of Solid State Physics, Lund University,
Lund 22100, Sweden

obtain the in situ temperature by Raman or SERS spectra because the very weak anti-Stokes peaks are generally hard to be observed experimentally.

In this letter, we report the experimental observation of ultrasensitive Stokes and anti-Stokes Raman peaks by our home-made HV-TERS system in a high-vacuum (10^{-7}Pa) condition. In order to collect more vibrational signals, the objective was put in the high-vacuum chamber, and focused onto the nano gap in the tip-substrate junction. The tunneling current and bias voltage can be controlled to vary the distance between the tip and substrate, further to change the local electromagnetic field enhancement. A gold tip with radius of about 50 nm was made by electrochemical etching of a 0.25-mm-diameter gold wire. The substrate was prepared by evaporating 100-nm silver film on a cleaned mica film under high vacuum.

Experiment

With our home-made HV-TERS, we have measured the Raman spectra of 1,2-benzenedithiol (1,2-BDT) on the silver film. The experimental processes are described as below. The substrate was firstly immersed in a 1,2-BDT (1×10^{-5}M) ethanol solution for 2 h, then washed with ethanol for 10 min to guarantee that there was only one monolayer of molecules adsorbed on the film. To reveal the advantages of HV-TERS than SERS in atmosphere, the typical SERS spectrum of 1,2-BDT in Ag sol and the normal Raman scattering (NRS) spectrum of 1,2-BDT powder were also measured with a Renishaw inVia Raman system in atmosphere and excited with light at 632.8 nm. It is found that the enhanced weak Stokes and anti-Stokes Raman peaks were clearly presented and the in situ experiment temperature was obtained from Stokes and anti-Stokes Raman spectra observed in HV-TERS.

Results and Disscusion

Figure 1a is the experimental HV-TERS spectrum of 1,2-BDT at the tunneling current of 1 nA and the bias voltage of 1 V. HV-TERS spectrum is much better than the SERS spectrum in Fig. 1b, especially in the region of low wavenumber. Obviously, the TERS spectrum has a stronger enhancement and a high signal-to-noise ratio compared with SERS spectrum. Furthermore, the closely neighbored C–C stretching modes at 1,540 and 1,561 cm^{-1} did not be resolved in SERS spectrum, which were clearly distinguished in the TERS spectrum.

To assign the Raman peaks in Fig. 1a, theoretical calculations were simulated by Gaussian 09 [19]. The ground state geometry of 1,2-BDT adsorbed on Ag cluster was optimized with density functional theory [20], B3LYP functional [21], 6-31G(D) basis set for S, C, H atoms, and LANL2DZ functional for Ag atom [22]. With the optimized geometry, the Raman spectrum of 1,2-BDT in Fig. 1d was done at the same level of theory. It can be found that the experimental and theoretical results are very consistent. Firstly, we assigned six strong Raman peaks A–F in Fig. 1 at the

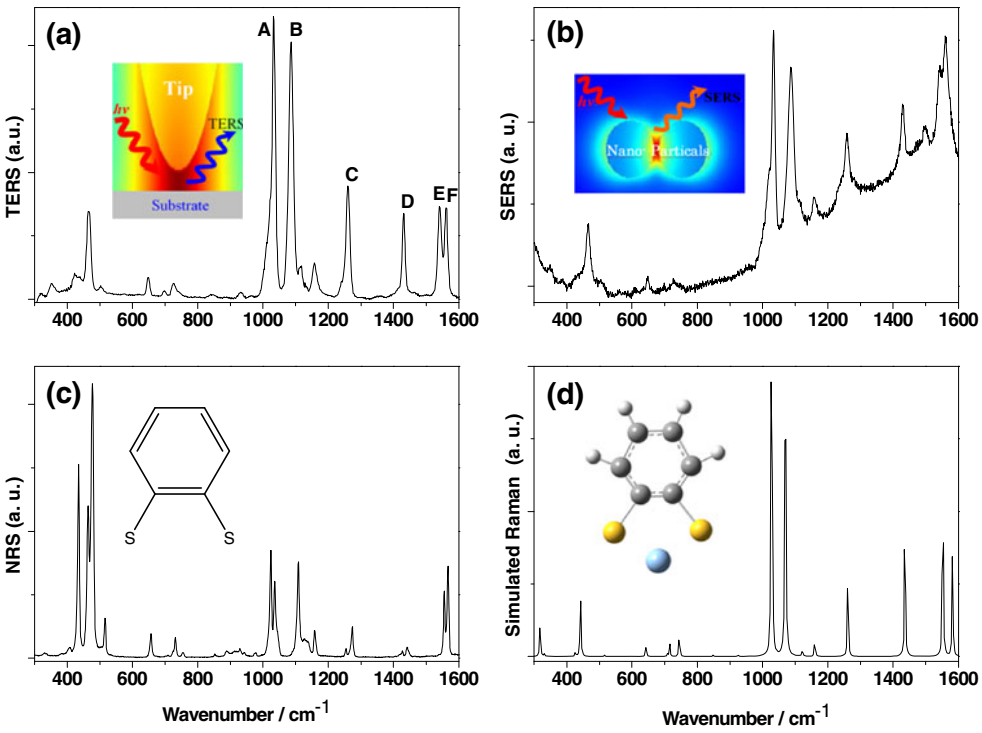

Fig. 1 **a** HV-TERS, **b** SERS, **c** NRS, and **d** simulated Raman spectra of 1,2-BDT. *Insets*: the schematics of TERS, SERS, molecular structure and simulated model, respectively

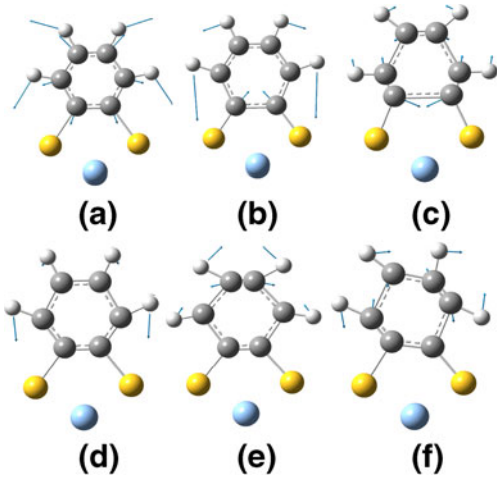

Fig. 2 The calculated Raman modes of 1,2-BDT adsorbed on Ag_2 cluster in Fig. 1a

region from 1,000 to 1,600 cm^{-1}, which can be seen in Fig. 2.

Secondly, we studied the weak Raman peaks in the range of low and high wavenumbers. Figure 3a is the HV-TERS spectrum at low wavenumber. It was found that many very weak Raman peaks can be observed clearly in the HV-TERS spectrum, which almost cannot be observed in SERS spectrum in Fig. 3c. These Raman peaks can be also clearly assigned theoretically and the vibrational modes can be seen from Fig. 4. It can be seen that the Raman peak b in Fig. 3a is the S–Ag vibrational mode of 1,2-BDT adsorbed on Ag substrate, which should not be observed in NRS spectrum of 1,2-BDT powder in Fig. 3e. Fig. 3b, d, and f are the HV-TERS, SERS and NRS spectra at high wavenumber around 3,000 cm^{-1}. It was found that only one of the three Raman peaks relative weak C–H vibrational modes can be observed in SERS spectrum, but all three peaks can be observed clearly in HV-TERS spectrum which is consistent with NRS spectrum. Comparing with the NRS spectra, such a shift of wavenumber in TERS and SERS spectra results from the interaction between the molecule and the metallic surface. Since the powder of 1,2-BDT were excited in Fig. 3e, f, the stronger NRS spectrum here was only a standard experiment spectrum for SERS and TERS spectra. HV-TERS spectrum was obtained from about one monolayer of 1,2-BDT molecules. Thus, ultrasensitive Raman signals can be obtained by our home-made HV-TERS system.

Meanwhile, we also measured Stokes and anti-Stokes HV-TERS spectra which are presented in Fig. 5. It is found that six Raman peaks were clearly observed in the anti-Stokes spectrum. The in situ local experimental temperature can be fitted with the Eq. 1,

$$I_s/I_{as} = a \times e^{(h\omega/k_B T)} \quad (1)$$

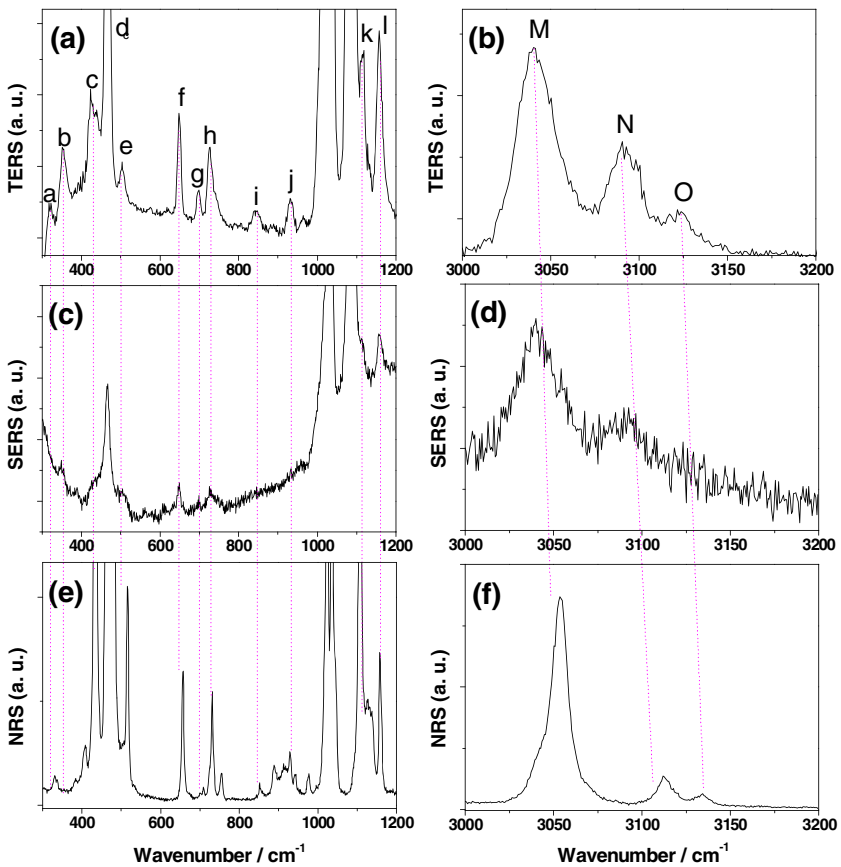

Fig. 3 HV-TERS spectra at the low (**a**) and high (**b**) wavenumber, compared with SERS spectra (**c**, **d**) and NRS spectra (**e**, **f**)

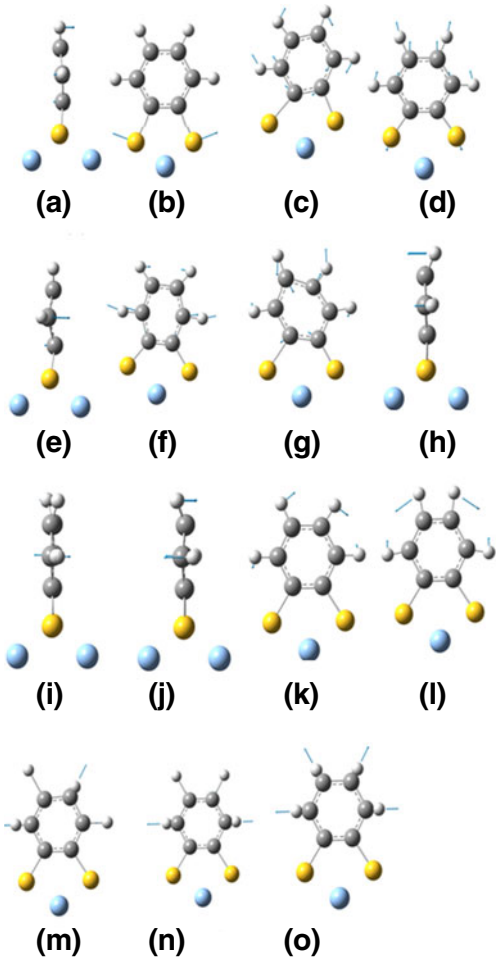

Fig. 4 The calculated Raman modes of 1,2-BDT adsorbed on Ag_2 cluster in Fig. 3**a** and **b**

where I_s and I_{as} are intensities of Stokes and anti-Stokes Raman signals, respectively; $\hbar$, k_B and T are Plank constant, Boltzmann constant and temperature, respectively. The a in Eq. (1) is an experimental parameter, which can be writen as,

$$a = \left(\frac{\sigma(\alpha_\omega)_{\text{Stokes}}}{\sigma(\alpha_\omega)_{\text{anti-Stokes}}}\right)\left(\frac{\omega_0 - \omega}{\omega_0 + \omega}\right)^{-4} \sum_{i=1}^{N} \frac{A^2_{\text{Stockes}}}{A^2_{\text{anti-Stockes}}} \quad (2)$$

where $\sigma(\alpha_\omega)_{\text{Stokes}}$ and $\sigma(\alpha_\omega)_{\text{anti-Stokes}}$ are frequency ω-dependent Stokes and anti-Stokes Raman scattering cross-section, respectively; ω_0 is the frequency of laser, N is the number of actived molecules, and $A^2_{\text{Stockes}}\left(A^2_{\text{anti-Stockes}}\right)$ are the enhancements of local fields in HV-TERS, including electromagnetic and chemical enhancements. In general, the enhancement can be site depedent and therefore should be summed over all active site. The calculated experimental temperature is 298(±6) K, and the experimental parameter a in Eq. (1) is 0.85 (±0.1).

Finally, we measured the laser polarization dependent HV-TERS spectra. The signal intensities of seven vibrational modes with polarization angle can be seen in Fig. 6a. It was found that the strongest Raman signals can be obtained with perpendicular incident polarization. To interpret the experimental results, theoretical simulation with finite-difference time-domain (FDTD) method was done using FDTD Solutions software [23]. The curve of electric field intensity in Fig. 6b as a function of incident polarization is well described by a simple sinusoidal dependence, which qualitatively agrees with experimental results. The near-field distributions were also plotted in logarithmic scale in the inset of Fig. 6b for perpendicular and parallel incident polarization. The intensity of the electric field with perpendicular incident polarization is much greater than that with parallel incident polarization. From the electromagnetic mechanism of TERS effect [12], we know that the best Raman signal can be

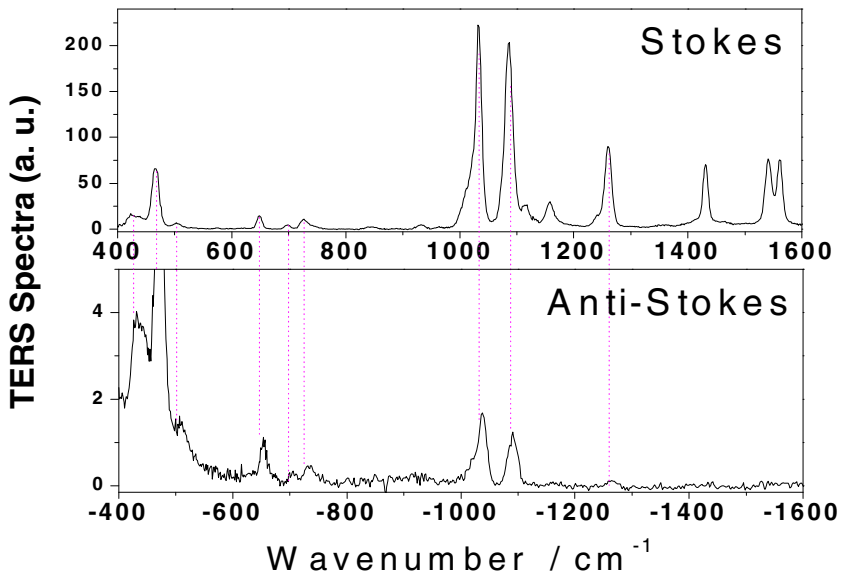

Fig. 5 The measured Stokes and anti-Stokes HV-TERS spectra

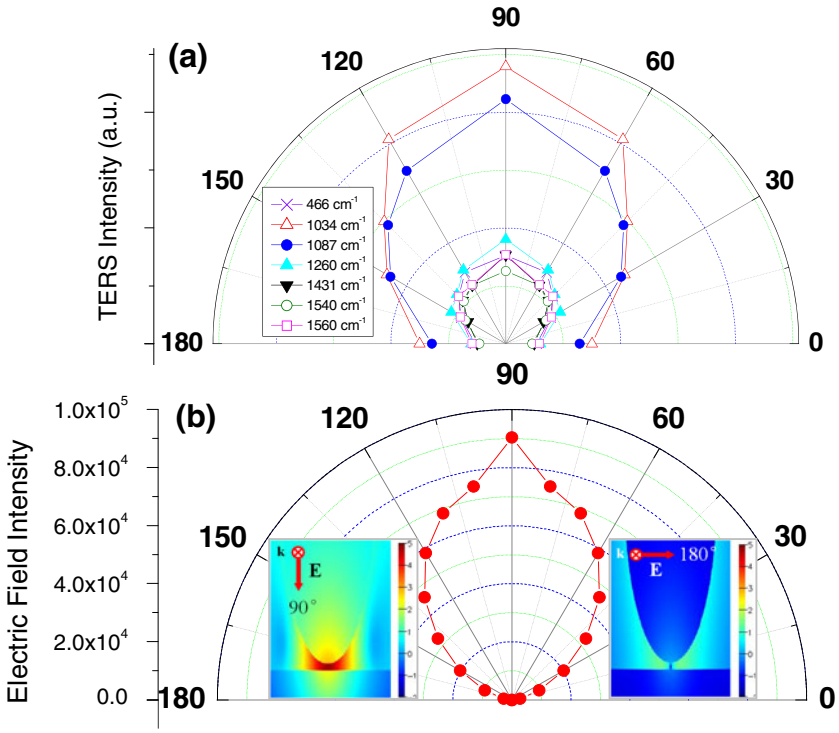

Fig. 6 The laser polarizati on dependent **a** measured HV-TERS intensity and **b** FDTD simulation electric field intensity. *Insets*: distributions of electric field intensity were plotted in logarithmic scale with perpendicular and parallel incident polarization

acquired with perpendicular incident polarization in our HV-TERS system.

Conclusion

In summary, we obtained ultrasensitive Stokes and anti-Stokes Raman spectra of 1,2-BDT adsorbed on Ag film with our home-made HV-TERS. Very weak Raman vibrational modes in Stokes and anti-Stokes Raman spectra were experimentally observed and assigned theoretically. The in situ experimental temperature was obtained by fitting the Stokes and anti-Stokes TERS spectra. These results demonstrate that the HV-TERS system can offer an effective new way for single molecular analysis, catalysis and synthesis molecules, electrochemistry, heterogeneous catalysis, and microelectronics beyond its excellent nanoscale optical analytical ability.

Acknowledgments This work was supported by the National Natural Science Foundation of China (grants 90923003, 10874234, 20703064 and 11174190), the National Basic Research Project of China (grant 2009CB930701), the Fundamental Research Funds for the Central Universities (no. 2010ZYGX025), and the Innovation Funds of Graduate Programs, SNU (no. 2010CXB004).

References

1. Stöckle M, Suh YD, Deckert V, Zenobi R (2000) Chem Phys Lett 318:131
2. Hayazawa N, Inouye Y, Sekkat Z, Kawata S (2000) Opt Commun 183:333
3. Anderson MS (2000) Appl Phys Lett 76:3130
4. Pettinger B, Ren B, Picardi G, Schuster R, Ertl G (2004) Phys Rev Lett 92:096101
5. Bailo E, Deckert V (2008) Chem Soc Rev 37:921
6. Steidtner J, Pettinger B (2008) Phys Rev Lett 100:236101
7. Chen JN, Yang WS, Dick K, Deppert K, Xu HQ, Samuelson L, Xu HX (2008) Appl Phys Lett 92:093110
8. Chan TS, Dvoynenko MM, Liu CY, Wang JK, Wang YL (2009) Opt Lett 34:2246
9. Sun MT, Fang YR, Zhang ZY, Xu HX (2012) arxiv:1112.4218v1 (in press)
10. Stadler J, Schmid T, Zenobi R (1856) Nanoscale 2012:4
11. Jiang N, Foley ET, Klingsporn JM, Sonntag MD, Valley NA, Dieringer JA, Seideman T, Schatz GC, Hersam MC, Van Duyne RP Nano Lett. doi:10.1021/nl2039925
12. Sun MT, Fang YR, Zhang ZY, Xu HX (2009) Phys Chem Chem Phys 11:9412
13. Yang ZL, Li QH, Fang YR, Sun MT (2011) Chem Commun 47:9131
14. Sun MT, Zang ZL, Zheng HR, Xu HX (2012) Sci. Rep. (in press)
15. Macfarlane RM, Hal Rosen, Seki H (1993) Solid State Commun 88:843
16. Evans CL, Xie XS (2008) Annu Rev Anal Chem 1:883
17. dos Santos DP, Andrade GFS, Brolo AG, Temperini MLA (2011) Chem Commun 47:7158
18. Deak JC, Iwaki LK, Rhea ST, Dlott DD (2000) J Raman Spectrosc 31:263
19. Frisch MJ (2009) Gaussian 09, Revision A.02, Gaussian, Inc., Wallingford CT
20. Hohenberg P, Kohn W (1964) Phys Rev 136:B864
21. Becke AD (1988) Phys Rev A 38:3098
22. Hay PJ, Wadt WR (1985) J Chem Phys 82:270
23. FDTD solutions, version 7.5 (2012) Lumerical Solutions, Inc.: Vancounver, British Columbia, Canada